Metrol. Meas. Syst., Vol. 26 (2019) No. 4, pp. 673–686
DOI: 10.24425/mms.2019.129586

METROLOGY AND MEASUREMENT SYSTEMS
Index 330930, ISSN 0860-8229
www.metrology.pg.gda.pl

ROBUST KALMAN FILTER-BASED FAULT-TOLERANT INTEGRATED BARO-INERTIAL-GPS ALTIMETER

Alberto Mañero Contreras[1)], Chingiz Hajiyev[2)]

1) *Politecnico di Milano, School of Industrial and Information Engineering, Via Raffaele Lambruschini, 15, 20156 Milano, Italy* (*amcamc92@gmail.com*)
2) *Istanbul Technical University, Aeronautics and Astronautics Faculty, 34467 Sarıyer, Istanbul, Turkey* (✉ *cingiz@itu.edu.tr*, +90 212 285 3105)

Abstract

As a result of the development of modern vehicles, even higher accuracy standards are demanded. As known, Inertial Navigation Systems have an intrinsic increasing error which is the main reason of using integrating navigation systems, where some other sources of measurements are utilized, such as barometric altimeter due to its high accuracy in short times of interval. Using a *Robust Kalman Filter* (RKF), error measurements are absorbed when a Fault Tolerant Altimeter is implemented. During simulations, in order to test the Nonlinear RKF algorithm, two kind of measurement malfunction scenarios have been taken into consideration; continuous bias and measurement noise increment. Under the light of the results, some recommendations are proposed when integrated altimeters are used.

Keywords: fault tolerance, robust Kalman filtering, integrated altimeter.

1. Introduction

Inertial Navigation Systems (INS) are ubiquitously employed to provide position and velocity measurements. However, measurements from INS gets degraded over time as INS errors are nonlinear and they are accumulated over time [1]. The errors can be divided into horizontal and vertical ones. Errors in the vertical channel directly contribute to malfunctions within altitude estimations. Joint measurements from external sources and INS ones are utilized to keep the vertical error growth within a predetermined bound.

Inertial and barometric altimeters gather diverse benefits and drawbacks [2–4]. The main reason to integrate these two navigators is primarily to combine the best features and remove the shortcomings. The principal advantages in the case of inertial altimeters are: the good features of the INS with high bandwidth and frequencies are maintained, in certain operation periods acceptable accuracy is attained and easily dynamic system adaptation to the computer environment is acquired. For the case of barometric altimeters, however, the benefits are: they give a high

accuracy, usually they are cheap and easy to implement, even though they need a recalibration periodically.

On the other hand, combining Global Positioning System and Inertial Navigation System has other advantages. Despite GPS measurements are typically less accurate than barometrical ones, it is also true that no recalibration of GPS sensor is needed depending on the flight day, in this case, because they always have the same mean error. In other words, measurements do not depend on pressure or temperature. The barometric altimeter augmented with integrated inertial GPS altimeter can provide more reliable and accurate navigation solutions under high maneuverings environments.

Reference [5] introduces an integrated navigation system based on a multi-sensor INS/GPS/Baro-altimeter. As known from the bibliography, the inertial errors grow exponentially and this effect is even more tangible when low-cost sensors are utilized. In order to restrain the aforementioned inaccuracy, a GPS receiver and a barometric altimeter are employed. The augmented system's vertical error is principally absorbed using the 3rd order vertical channel damping loop and the application of the adaptive error damp coefficients. This integration is done with an *extended Kalman filter* (EKF).

In [6] Model Aided Inertial Navigation has been used for the UAV automatic landing system. The integrated measurement system presented in this work can estimate the UAV altitude using the ground effect.

In [7], three integrated systems have been considered: baro-inertial, inertial-GPS and baro-inertial-GPS. An optimal Kalman filter has been implemented in the design of them. According to this study, pressure-based measurements are more accurate than those ones calculated through GPS. However, when all the signals are multiplexed, the final output is better than both sources separately. This is the main and most important conclusion of this analysis. The integrated altimeters which described in [5–7] are not robust to the sensor faults. The fault-tolerant properties of the aforementioned integrated systems are not provided in this study.

The fault-tolerant integrated altimeter, comprising of the radar and inertial altimeters is discussed in [8]. The integration is performed via Nonlinear Robust Adaptive Kalman Filter having real-time correction of its filter gain coefficients. It is based on the assessment of the posterior probability of the normal operation of altimeter using current altitude measurement. In conclusion, faults in the integrated altimeter are corrected by the proposed algorithm, without affecting the good estimation altitude behavior.

The integrated navigation systems with application of multi-height sensor data fusion and fault tolerant estimation procedure are presented in [9]. In this study at first for the altitude sensors fault detection problem is fulfilled in real time. Then data fusion is completed by using fault tolerance in real time. Fault tolerant altimeter architecture has been designed by using three sub-filters corresponding to the GPS, baro- altimeter and radar altimeter.

In the present research, three different fault tolerant Integrated altimeters have been analyzed: *integrated baro-inertial* (IBI), *integrated inertial-GPS* (IIG) and *integrated baro-inertial-GPS* (IBIG). The first and the second are designed through a *complementary Kalman filter* (CKF). When some random faulty cases are introduced in the measuring system, the *Robust Kalman Filter* (RKF) case is considered. The fault-tolerant integrated IBI, IIG and IBIG altimeters based on the developed RKF are proposed and compared with the conventional integrated altimeters.

2. Integrated altimeter design

Because of its outstanding characters such as high-accuracy, self-contained and jam-proof, the INS has become the core of navigation systems for most vehicles. Nevertheless, Inertial

Metrol. Meas. Syst., Vol. 26 (2019), No. 4, pp. 673–686
DOI: 10.24425/mms.2019.129586

Navigation Systems suffer from an increasing error as stated before. Hence, this fact justifies the use of integrated navigation systems, where some other sources of measurements are utilized, such as barometric altimeter due to its high accuracy in tight time intervals. First, it is needed to show the error models of the inertial, barometric and GPS altimeters. Every single model has an unavoidable error. In this section, these error models are presented.

2.1. Error models

The barometric altimeter's measuring model used in this research includes the bias error of the first order Markov process and a random white Gaussian noise as stated in [5], being expressed in the next equations:

$$h_B = h_T + B + v_B\,, \tag{1}$$

$$\dot{B} = -\frac{1}{\tau}B + U_B\,, \tag{2}$$

being h_B the altitude output from the barometer; h_T represents the true height, measurement noise is taken into account by v_B; τ is the bias error's B correlation time and U_B compounds the white Gaussian noise.

Due to the large variety of outputs from diverse channels, the INS carries a complex error model. In this study, the main parameter that simulations are focused at is the vertical altitude error. The linear, discrete error model of the vertical INS channel is given by [10]:

$$\Delta H_I(i) = \Delta H_I(i-1) + T_d \Delta W_z(i-1), \tag{3}$$

$$\Delta W_z(i) = \Delta W_z(i-1) + \frac{2gT_d}{R_I}\Delta H_I(i-1) + T_d \Delta a_z(i-1) + T_d \Delta g(i-1), \tag{4}$$

$$\Delta a_z(i) = \Delta a_z(i-1) - T_d \alpha \Delta a_z(i-1) + T_d U_{\Delta a_z}(i-1), \tag{5}$$

$$\Delta g(i) = \Delta g(i-1) - T_d \beta_g \Delta g(i-1) + T_d U_{\Delta g}(i-1), \tag{6}$$

where: $\Delta W_z(i-1)$ and $\Delta H_I(i)$ represent the measurement errors of the vertical speed and the altitude; $\Delta a_z(i-1)$ and $\Delta g(i-1)$ are the measurement errors of the vertical acceleration and the gravitational acceleration; $U_{\Delta a_z}(i-1)$ and $U_{\Delta g}(i-1)$ are the white Gaussian noises with zero mean, α and β_g are the terms used for the correlation period, T_d is the sampling time; $R_I = R_0 + H$, H is the flight altitude and R_0 is the radius of Earth.

For the case of GPS error model, a Gaussian random white noise error has been taken, with zero mean and without bias.

2.2. Scheme 1: Integrated Baro-Inertial altimeter

As known [3], information provided by the inertial channel gets inaccurate over time ever since the errors are accumulated growing exponentially. The errors can be separated into horizontal and vertical errors. Errors in the vertical channel directly contribute to malfunctions in altitude estimations. Joint measurements from other external navigation systems and INS ones are used to keep the vertical channel error growth within bounds. The schema of the proposed IBI altimeter structure is presented in Fig. 1.

The *central processing unit* (CPU) block is necessary because of the existent discrepancy in altitude references between the barometrical altimeter the inertial one, measuring the former

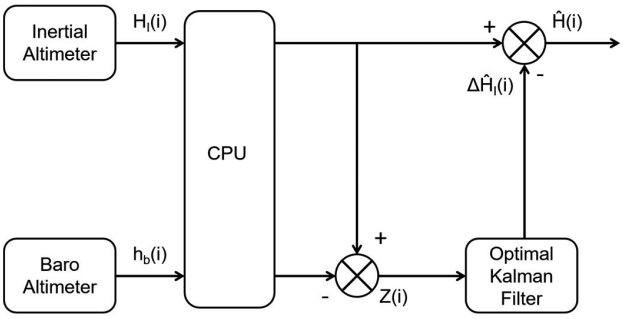

Fig. 1. Schema of the IBI altimeter structure.

from sea level conditions and the latter from a set up initial alignment location. In a system where measurements are not coherent because of the sensors combination, the dissimilarity in altitudes can be adjusted via Central Processing Unit. The measurement matrix for this system in order to be consistent with the theory aforementioned explined is:

$$H_{IBI}(k) = \begin{bmatrix} 1 & 0 & 0 & 0 & -1 \end{bmatrix}. \tag{7}$$

The scheme shown in Fig. 1 symbolizes the acquiring process of vertical measurements when baro-inertial altimeter is used. For these integrated systems, the state vector proposed is:

$$X^T(i) = \begin{bmatrix} \Delta H_I(i) & \Delta W_z(i) & \Delta a_z(i) & \Delta g(i) & B(i) \end{bmatrix}, \tag{8}$$

where $B(i)$ represents the baro-altimeter bias error. The state space model of the integrated baro-inertial altimeter could be expressed through the following equations:

$$X(i) = \varphi(i, i-1)X(i-1) + G(i, i-1)U(i-1), \tag{9}$$

$$Z(i) = H_{IBI}(i)X(i) + V(i), \tag{10}$$

being $\varphi(i, i-1)$ the system transition matrix, $G(i, i-1)$ represents the system noise transition matrix; $Z(i)$ is the measurement vector, $V(i)$ is the white Gaussian measurement noise vector, and $U^T(i-1) = [\, U_{\Delta a_z}(i-1) \;\; U_{\Delta g}(i-1) \;\; U_B(i-1)], \,]$ is the white Gaussian system noise vector. The index $(i, i-1)$ in transition matrix shows the transition of the system from time $i-1$ to time k time). The matrices $\varphi(i, i-1)$ and $G(i, i-1)$ are defined as follows:

$$\varphi(i, i-1) = \begin{bmatrix} 1 & T_d & 0 & 0 & 0 \\ \dfrac{2gT_d}{R_I} & 1 & T_d & \Delta t & 0 \\ 0 & 0 & 1-\alpha T_d & 0 & 0 \\ 0 & 0 & 0 & 1-\beta_g T_d & 0 \\ 0 & 0 & 0 & 0 & 1-\beta T_d \end{bmatrix}, \tag{11}$$

Metrol. Meas. Syst., Vol. 26 (2019), No. 4, pp. 673–686
DOI: 10.24425/mms.2019.129586

where $\beta = \dfrac{1}{\tau}$ is the inverse correlation time of the bias error B,

$$G(i, i-1) = \begin{bmatrix} 0 & 0 & 0 \\ 0 & 0 & 0 \\ T_d & 0 & 0 \\ 0 & T_d & 0 \\ 0 & 0 & T_d \end{bmatrix}, \tag{12}$$

$$R(i) = \sigma^2_{H_I} + \sigma^2_{H_B}\,. \tag{13}$$

2.3. Scheme 2: Integrated Inertial GPS altimeter

There are many cases in which appliance of integrated inertial GPS altimeters is common. To integrate the above mentioned navigation systems an Indirect Kalman filtering technique is utilized. The measurement matrix of the integrated altimeter for this case is:

$$H_{IIG}(i) = \begin{bmatrix} 1 & 0 & 0 & 0 & 0 \end{bmatrix}. \tag{14}$$

In this case, the last value is set to zero because GPS bias error has not been taken into consideration for this integrated inertial GPS altimeter. The state vector proposed is:

$$X^T(i) = \begin{bmatrix} \Delta H_I(i) & \Delta W_z(i) & \Delta a_z(i) & \Delta g(i) \end{bmatrix}. \tag{15}$$

The system transition matrix $\varphi(i, i-1)$ and system noise transition matrix $G(i, i-1)$ are defined in this case as follows:

$$\varphi(i, i-1) = \begin{bmatrix} 1 & T_d & 0 & 0 \\ \dfrac{2gT_d}{R_I} & 1 & T_d & T_d \\ 0 & 0 & 1-\alpha T_d & 0 \\ 0 & 0 & 0 & 1-\beta_g T_d \end{bmatrix}, \tag{16}$$

$$G(i, i-1) = \begin{bmatrix} 0 & 0 \\ 0 & 0 \\ T_d & 0 \\ 0 & T_d \end{bmatrix}, \tag{17}$$

$$R(i) = \sigma^2_{H_I} + \sigma^2_{H_G}\,. \tag{18}$$

2.4. Scheme 3: Integrated Baro-Inertial GPS altimeter

The integrated inertial GPS altimeter is designed using a loosely coupled integration architecture that incorporates a GPS navigation solution. Due to atmospheric effects and satellite's geometry, the GPS vertical channel typically has a poor accuracy.

By augmenting the barometric altimeter measurements, the vertical channel can be stabilized under GPS faulty conditions. The flight data results show that the baro-altimeter augmented IIG

altimeter can provide more reliable and accurate height measurements. The structure scheme of the integrated baro-inertial-GPS altimeter is given in Fig. 2 [7]. As shown, the measurements obtained by the sensors pass through local filters and then arrive at the integration block. Here, they are fused via data fusion algorithm before providing the estimation of the altitude to the user.

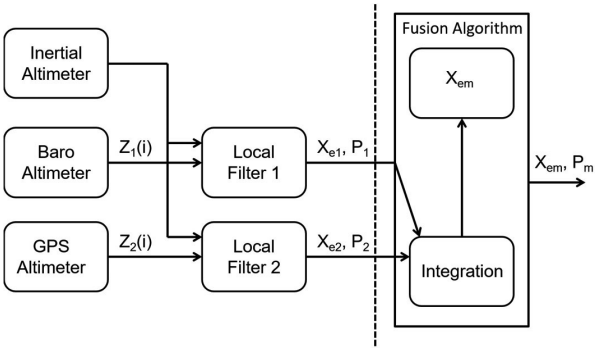

Fig. 2. IBIG altimeter structure scheme.

The data fusion algorithm is used for fusing the measurements in the IBIG altimeter is:

$$\Delta H_{IBIG} = \frac{Var\,(\Delta H_{IBI})\Delta H_{IIG} + Var\,(\Delta H_{IIG})\Delta H_{IBI}}{Var\,(\Delta H_{IBI}) + Var\,(\Delta H_{IIG})}, \tag{19}$$

$$Var\,(\Delta H_{IBIG}) = \left[\frac{1}{Var\,(\Delta H_{IBI})} + \frac{1}{Var\,(\Delta H_{IIG})}\right]^{-1} = \frac{Var\,(\Delta H_{IBI})Var\,(\Delta H_{IIG})}{Var\,(\Delta H_{IBI}) + Var\,(\Delta H_{IIG})}, \tag{20}$$

where: ΔH_{IBIG} is the IBIG altimeter error; $Var\,(\Delta H_{IBI})$ and $Var\,(\Delta H_{IIG})$ are the variances of the IBI and IIG altimeters errors respectively; $Var\,(\Delta H_{IBIG})$ is the variance of the IBIG altimeter error.

Hence, the altitude estimation value can be determined as:

$$\hat{H}_{IBIG}(i) = H_I(i) - \Delta\hat{H}_{IBIG}(i). \tag{21}$$

3. Kalman filtering for the integration of altimeters

As known, the *optimum Kalman filter* (OKF) is a linear filter, and the actual differential equations for INS errors are nonlinear. Therefore, in OKF applications the INS error model is valid for linearized version. So the requirements for the errors is to remain small. The equations of the Kalman filter in its general form is presented below.

3.1. Optimal Kalman filter for the integration of altimeters

The state space model used throughout this study is expressed by (8)–(9). For the estimation of the states of the system (8), the following statements are the Kalman equations to be used. The equation of the estimation value on the iteration i is:

$$\hat{X}(i/i) = \hat{X}\,(i/i-1) + K(i)\Delta(i), \tag{22}$$

Metrol. Meas. Syst., Vol. 26 (2019), No. 4, pp. 673–686
DOI: 10.24425/mms.2019.129586

being $K(i)$ the Kalman gain matrix and $\Delta(i)$ represents an innovation sequence defined in the following lines taken from [8]. The variable $\hat{X}(i/i-1)$ estimates the extrapolation value of the space state vector. The first element of the double index shows the time instant in which the parameter is estimated, and second one – number of measurements on which the estimation is carried out. The expressions of these three variables are:

$$\hat{X}(i/i-1) = \varphi(i, i-1)\hat{X}(i-1/i-1), \tag{23}$$

$$\Delta(i) = Z(i) - H(i)\hat{X}(i/i-1), \tag{24}$$

$$K(i) = P(i/i-1)H^T(i)\left[H(i)P(i/i-1)H^T(i) + R(i)\right]^{-1}, \tag{25}$$

where $R(i)$ is the covariance matrix of measurement noise. On the other hand, matrixes $P(i/i)$ and $P(i/i-1)$ represent covariance matrixes of estimation and extrapolation errors, which respectively have the following form:

$$P(i/i) = [I - K(i)H(i)]\,P(i/i-1), \tag{26}$$

$$P(i/i-1) = \varphi(i, i-1)P(i-1/i-1)\varphi^T(i, i-1) + G(i, i-1)Q(i-1)G^T(i, i-1), \tag{27}$$

where $Q(i-1)$ is the covariance matrix of system noise. The software used to implement these algorithms has been MATLAB.

3.2. Robust Kalman Filter

Throughout this paper, a *Robust Kalman Filter* (RKF) is proposed since it deals in a better way with abrupt fault cases in the estimation system such as computer malfunctions, abnormal measurements or noise increments, which are all described in the next section. The equation of the estimation value is [8]:

$$\hat{X}(i/i) = \hat{X}(i/i-1) + prob\,(1/i)K(i)\Delta(i). \tag{28}$$

Here $prob\,(1/i)$ is the posterior probability of the normal operation of the estimation system, given for measurement results at the i^{th} time step. The other parameters have been already defined in the last section. When $prob\,(1/i) = 1$, this filter will be exactly the same as the OKF, but when $prob\,(1/i) \neq 1$ a new calculation in order to estimate the variables of interest is done. During normal operation of the measurement channel, $\widetilde{\Delta}(k)$ normalized innovation sequence of *Kalman Filter* is:

$$\widetilde{\Delta}(i) = \left[H(i)P(i/i-1)H^T + R(i)\right]^{-1/2}\Delta(i), \tag{29}$$

will satisfy the normal distribution $N(0, 1)$. Consequently, the adaptative filtration algorithm with the filter gain matrix correction can be presented in the form below:

$$\hat{X}(i/i) = \hat{X}(i/i-1) + K_A(i)\Delta(i), \tag{30}$$

$$K_A(i) = prob\,(1/i)K(i), \tag{31}$$

$$prob\,(1/i) = \frac{1}{\sqrt{2\pi}\sigma_{\widetilde{\Delta}}(i)}\int_{-3}^{3}\exp\left\{-\frac{\left[\widetilde{\Delta}(i) - \hat{\widetilde{\Delta}}(i)\right]^2}{2\sigma^2_{\widetilde{\Delta}}(i)}\right\}d\widetilde{\Delta}. \tag{32}$$

The rest of the equations and parameters have been already defined throughout the last section. If the posterior probability $prob\,(1/i)$ changes, then the gain coefficient of the robust filter $K_R(i)$ is automatically changed. Calculating the integral defined earlier, it gives to the Kalman Filter the ability to adapt to change in operating conditions [11]. If there is a fault in the measurement channel, the value $prob\,(1/i)$ decreases, and the gain coefficient of the filter decreases too. Therefore, the correction effect of innovation sequence decreases and the estimated $\hat{X}(i/i)$ approaches to the extrapolation value $\hat{X}(i/i-1)$.

4. Simulations

In order to test the proposed OKF and RKF algorithms in the current section, the sensor malfunction scenarios are examined. The continuous bias, and measurement noise increment type sensor faults are taken into consideration. The following simulation scenarios are investigated in this study: Integrated baro-inertial altimeter; Integrated inertial-GPS altimeter; Integrated baro-inertial-GPS altimeter. The simulations are performed on programming language "MATLAB" using the parameters given in Table 1 [7].

Table 1. Values of parameters used in simulations.

Variable	Value	Units	Definition
Δt	0.5	s	Discrete time
R_0	6378150	m	Radius of the Earth
H	1000	m	Flight altitude
g	9.81	m/s^2	Gravitational acceleration
β	0.01	s^{-1}	Term of the correlation period
β_g	0.005	s^{-1}	Term of the correlation period
α	0.001	s^{-1}	Term of the correlation period
σ_w	0.0001	m/s	Vertical speed white noise standard deviation
$\sigma_{\Delta az}$	0.00002	m/s^2	Vertical acceleration white noise standard deviation
$\sigma_{\Delta g}$	0.00002	m/s^2	Gravitational acceleration white noise standard deviation
σ_B	1	m	Baroaltimeter error standard deviation
σ_{INS}	3	m	Inertial system vertical channel error standard deviation
σ_{GPS}	2.23	m	GPS vertical error standard deviation

The following fault-free simulation scenarios are investigated in this study:
- Fault-free scenario 1: Integrated baro-inertial altimeter;
- Fault-free scenario 2: Integrated inertial-GPS altimeter;
- Fault-free scenario 3: Integrated baro-inertial-GPS altimeter.

4.1. Definition of faulty cases

4.1.1. Continuous bias at measurements

Continuous bias term is created by adding a constant term to the measurement channel between the 200th and 400th iteration. As a result, the measured error is displaced upwards stepwise because of the added positive constant. The abbreviation for this faulty case is CBM.

Metrol. Meas. Syst., Vol. 26 (2019), No. 4, pp. 673–686
DOI: 10.24425/mms.2019.129586

4.1.2. Measurement noise increment

Finally, the last measurement error is based on noise increments. In this measurement malfunction scenario, measurement fault is characterized by multiplying the variance of the measurement noise by a constant term between 200th and 400th iteration. The effect of this error is an amplification on the noises. The abbreviation for this faulty case is MNI.

4.1.3. Faulty case scenarios

The following faulty simulation scenarios are investigated below:

Faulty Case Scenario 1: IBI and IIG altimeters are performing in MNI faulty case;

Faulty Case Scenario 2: IBI altimeter is operating in CBM mode and the IIG altimeter is measuring in normal conditions;

Faulty Case Scenario 3: IBI and IIG altimeters are performing in CBM faulty case;

Faulty Case Scenario 4: IBI altimeter is operating in MNI mode and the IIG altimeter is measuring in normal conditions;

Faulty Case Scenario 5: IBI altimeter is operating in MNI mode and the IIG altimeter in CBM mode.

4.2. The error of estimating the error

It should be underlined that, the integration algorithm here in this study is based upon error models and error values. The use of the system designed in this study is to find out instantaneous errors at the integrated altimeter. So the discrimination between navigation error and filter error is somehow very important. The error definition in the results is standing for *the error of finding the error*. As the system design is mainly based on Kalman filter, it will be more convenient to express this definition as *the error of estimating the error*.

4.3. Integrated altimeters simulation results (fault free case)

In this section, the main output of this fused integrated navigation system is shown. Due to the visual similarity with previous results, only the behaviours of the altitude errors are given. The simulation results are presented in the Fig. 3.

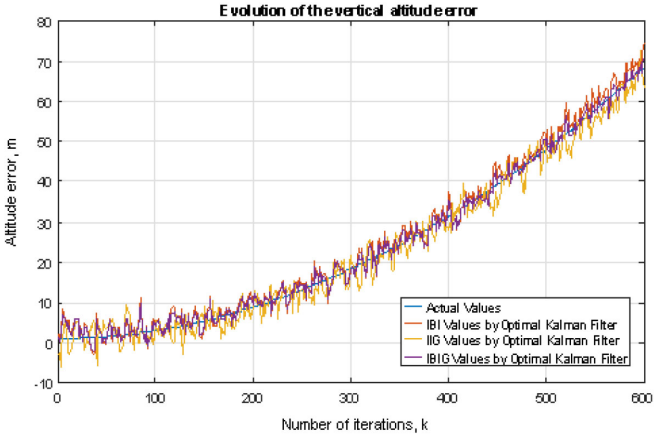

Fig. 3. Altitude measurements comparison between altimeters.

The largest errors are seen on IIG altimeter which is one of the three altimeters. The second largest errors give the IBI altimeter and finally, the best results are obtained by the fused IBIG altimeter, as expected. In the Table 2 are shown the mean error of estimating the error for all the cases, verifying the visual results. The standard deviation of error of estimating the error is given in Table 2. As seen from the presented results, the standard deviation of the IBIG altimeter error is the smallest.

Table 2. Comparison between altimeters in altitude measurements.

Altimeter	**Mean Error of Estimating the Error [m]**	**Standard Deviation of the Error [m]**
Baro-Inertial (IBI)	1.87	0.0418
Inertial-GPS (IIG)	2.17	0.0588
Baro-Inertial-GPS (IBIG)	1.43	0.0165

4.4. Faulty case Scenario 1

The first experiment has been run when both channels are performing in MNI faulty case. The results obtained are presented in Fig. 4. As can be checked in Table 3, the mean error of estimating the error and the standard deviation of the error obtained for the IBIG system are much better than the ones calculated for each integrated system separately.

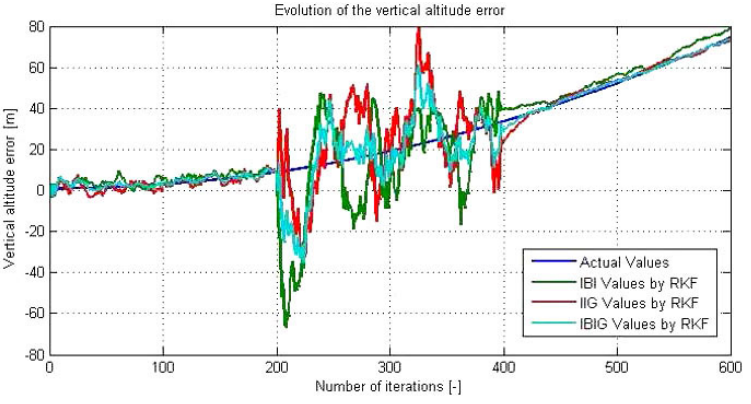

Fig. 4. Results of Scenario 1.

Table 3. Mean Errors of Scenario 1.

Integrated Altimeter	**Mean Error of Estimating the Error [m]**	**Standard Deviation of the Error [m]**
Baro-Inertial (IBI)	9.37	0.4376
Inertial-GPS (IIG)	6.27	0.2392
Baro-Inertial-GPS (IBIG)	4.45	0.2009

Metrol. Meas. Syst., Vol. 26 (2019), No. 4, pp. 673–686
DOI: 10.24425/mms.2019.129586

4.5. Faulty case Scenario 2

The second experiment has been performed when the IBI altimeter is operating in CBM mode and the IIG altimeter is measuring in normal conditions. The result is depicted in Fig. 5. As shown, the fused integrated system absorbs partially the errors introduced by the IBI altimeter, and the mean error of estimating the error and the standard deviation of the error are presented in Table 4.

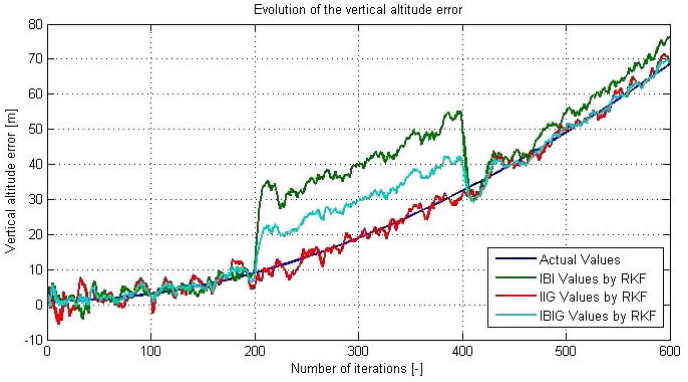

Fig. 5. Results of Scenario 2.

Table 4. Mean Errors of Scenario 2.

Integrated Altimeter	**Mean Error of Estimating the Error [m]**	**Standard Deviation of the Error [m]**
Baro-Inertial (IBI)	7.54	0.2734
Inertial-GPS (IIG)	1.25	0.0920
Baro-Inertial-GPS (IBIG)	4.61	0.1849

As seen from Table 4, IBIG results are worse than the results in the non-faulty altimeter.

4.6. Faulty case Scenario 3

The third experiment has been done when both channels are performing in CBM faulty case. The results when both channels are performing continues bias type faulty case between of 200–400th iterations are presented in Fig. 6. Mean error of estimating the error and the standard deviation of the error for the Scenario 3 are given in Table 5.

Table 5. Mean Errors of Scenario 3.

Integrated Altimeter	**Mean Error of Estimating the Error [m]**	**Standard Deviation of the Error [m]**
Baro-Inertial (IBI)	7.57	0.3587
Inertial-GPS (IIG)	7.54	0.3577
Baro-Inertial-GPS (IBIG)	7.28	0.3473

As seen in Table 5, IBIG results are better than the results in the both faulty altimeters.

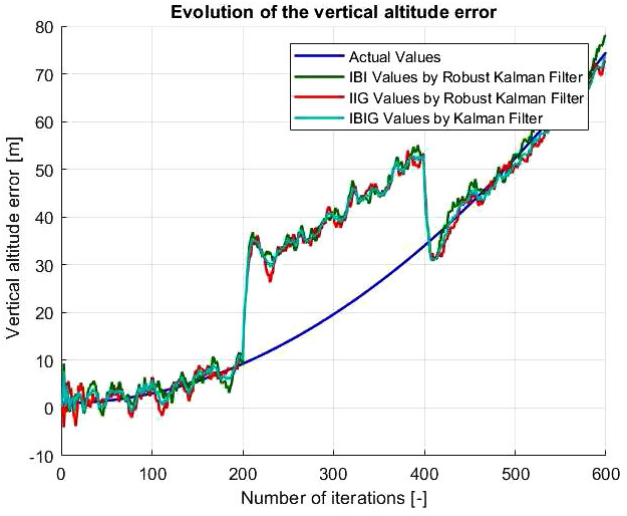

Fig. 6. Results of Scenario 3.

4.7. Faulty case Scenario 4

The fourth experiment has been performed when the IBI altimeter is operating in MNI mode and the IIG altimeter is measuring in normal conditions. The result when the IBI altimeter is operating in MNI mode between of 200–400th iterations and the IIG altimeter is measuring in normal conditions are depicted in Fig. 7. The mean error of estimating the error and the standard deviation of the error for this case are presented in Table 6.

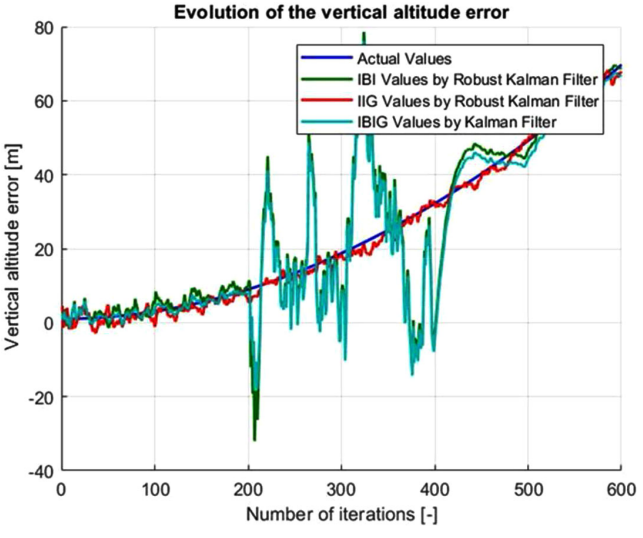

Fig. 7. Results of Scenario 4.

As seen in Table 6, IBIG results are worse than the results in the non-faulty altimeter.

Metrol. Meas. Syst., Vol. 26 (2019), No. 4, pp. 673–686
DOI: 10.24425/mms.2019.129586

Table 6. Mean Errors of Scenario 4.

Integrated Altimeter	Mean Error of Estimating the Error [m]	Standard Deviation of the Error [m]
Baro-Inertial (IBI)	6.72	0.3687
Inertial-GPS (IIG)	1.27	0.0279
Baro-Inertial-GPS (IBIG)	6.15	0.3437

4.8. Faulty case Scenario 5

The fifth experiment consists when the IBI altimeter is operating in MNI mode and the IIG altimeter in CBM mode. The results are presented in Fig. 8 and Table 7.

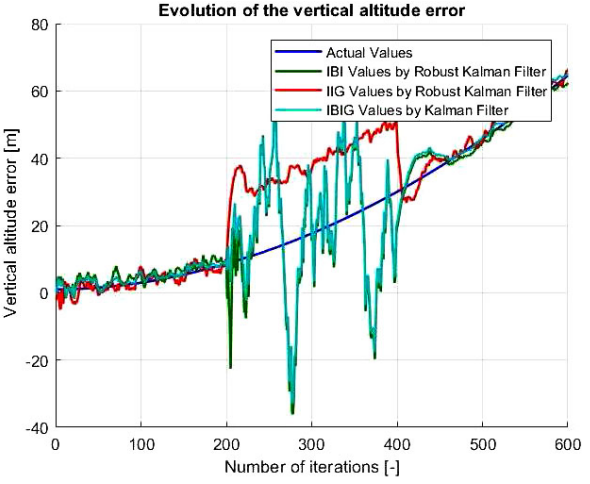

Fig. 8. Results of Scenario 5.

Table 7. Mean Errors of Scenario 5.

Integrated Altimeter	Mean Error of Estimating the Error [m]	Standard Deviation of the Error [m]
Baro-Inertial (IBI)	6.59	0.2370
Inertial-GPS (IIG)	7.54	0.3075
Baro-Inertial-GPS (IBIG)	5.62	0.1979

As can be checked in Table 7, the mean error of estimating the error and the standard deviation of the error obtained for the IBIG system are better than the ones calculated for each integrated system separately.

5. Conclusions

This study presents a fault-tolerant integrated Baro-Inertial-GPS altimeter based on Nonlinear RKF algorithm. Integration is performed using a complementary Kalman filter with correction

of its filter gain coefficients. The faulty measurements are considered with small weights and the proposed RKF compensates for erroneous results by reducing the values of the filter gain coefficients.

In the demonstrations, two type of integrated altimeters are implemented and compared: OKF based and RKF based. During simulations, two kinds of sensor malfunction scenarios are examined; continuous bias and measurement noise increment. In faulty scenarios, the accuracy of OKF based integrated altimeters are worse than the other method. When fault occurs on the measurements, the accuracy of RKF based integrated altimeters are considerably better than the accuracy of the conventional OKF based altimeters.

As a result, the following recommendations for the use of integrated altimeters have been proposed:

- In the fault free case the conventional OKF based IBIG altimeter can be preferred.
- If one of the integrated altimeters (IBI or IIG) is faulty, it is proposed to use the fault-free integrated altimeter instead of the IBIG altimeter, because in this case, IBIG altimeter accuracy is worse than the fault-free integrated altimeter accuracy.
- If both of integrated altimeters are faulty, then the RKF based IBIG altimeter provides better altitude accuracy and it is preferred.

References

[1] Kayton, M., Fried, W.R. (1997). *Avionics navigation systems*. 2nd ed., New York: John Willey & Sons, Inc.

[2] Hajiyev, C., Saltoglu, R. (2004). RKF-based fault tolerant integrated INS/radar altimeter. *Aircraft Engineering and Aerospace Technology: An International Journal*, 76(1), 38–46.

[3] Rogers, R.M. (2007). *Applied Mathematics in Integrated Navigation Systems*. 3rd ed., Reston, VA, USA, American Institute of Aeronautics and Astronautics, Inc.

[4] Hajiyev, C. (2007). Adaptive filtration algorithm with the filter gain correction applied to integrated INS/radar altimeter. *Proc. of the Institution of Mechanical Engineers (IMechE), Part G, Journal of Aerospace Engineering*, 221, 847–855.

[5] Sokolovic, V., Dikic, G., Stancic, R. (2014). Adaptive error damping in the vertical channel of the INS/GPS/Baro-altimeter integrated navigation system. *Scientific Technical Review*, 64(2), 14–20.

[6] Nobahari, H., Mohammadkarimi, H. (2017). Application of model aided inertial navigation for precise altimetry of Unmanned Aerial Vehicles in ground proximity. *Aerospace Science and Technology*, 69, 650–658.

[7] Contreras, A.M., Hajiyev, C. (2018). Integration of baro-inertial-GPS altimeter via complementary Kalman filter. Karakoç T., Colpan C., Şöhret Y. (eds). *Advances in Sustainable Aviation. Springer, Cham*, 251–268.

[8] Hajiyev, C. (2012). Fault tolerant integrated radar/inertial altimeter based on nonlinear robust adaptive Kalman filter. *Aerospace Science and Technology*, 17(1), 40–49.

[9] Geng, K.K., Chulin, N.A. (2017). Applications of multi-height sensors data fusion and fault-tolerant Kalman filter in integrated navigation system of UAV. *Procedia Computer Science*, 103, 231–238.

[10] Zhukovskiy, A.P., Rastorguev, V.V. (1998). *Complex Radio Navigation and Control Systems of Aircraft*. Moscow: MAI.

[11] Contreras,A.M., Hajiyev, C. (2019). Comparison of Conventional and Robust Adaptive Kalman Filters Based Integrated Altimeters. *Proc. of the 20th International Carpathian Control conference (ICCC-2019)*, Wieliczka, Poland, May, 2019, *IEEE*, 6.